18.2 CMOS-Driven Pneumatic-Free Scalable Microfluidics and Fluid Processing with Label-Free Cellular and Bio-Molecular Sensing Capability for an End-to-End Point-of-Care System

Chengjie Zhu, Jesus Maldonado, Hao Tang, Suresh Venkatesh, Kaushik Sengupta

Princeton University, Princeton, NJ

2021 IEEE International Solid- State Circuits Conference (ISSCC) | 978-1-7281-9549-0/20/$31.00 ©2021 IEEE | DOI: 10.1109/ISSCC42613.2021.9365843

The emergence of the pandemic has demonstrated the necessity of point-of-care (POC) molecular diagnostic platforms that encompass an end-to-end system (from sample fluid to diagnostic information) with the ability to allow rapid analysis on the spot. While POC sensing technologies have been demonstrated in miniaturize chip-scale platforms [1-5], the bottlenecks in enabling end-to-end low-cost handheld platforms have often been bio-sample handling, filtering, mixing with re-agents that are critical to the robustness of the assay chemistry and sensing sensitivity/specificity. These processes are typically carried out either manually or by employing complex pneumatic flow control with multiple bulky syringe pumps, which have been a severe limitation to enable end-to-end biosensing systems (Fig. 18.2.1). While electrically driven droplets, molecular and cell manipulation techniques, such as electro-wetting, electrophoresis and dielectrophoresis, have been demonstrated in singular systems before [1], they do not have the ability to process bulk bio-sample fluids that is required for POC devices. In this paper, we present a scalable approach that merges the functionalities of sample processing and cellular/bio-molecular sensing in a single system and eliminates any pneumatic pumping mechanisms by exploiting CMOS-based electrically driven electro-kinetic flow of bulk fluids. We demonstrate, for the first time, a CMOS-microfluidic system that is capable of 1) pumping bulk electrolyte fluid with AC electro-osmosis, 2) cell manipulation and separation with dielectrophoresis (DEP), 3) label-free bio-molecular and cell sensing, classification with dedicated 16-element impedance spectroscopy receivers. While we demonstrate these kernel functionalities in a multi-chip module/microfluidic interface (Fig. 18.2.1), the overall architecture, fluidics and sensing components can be massively scaled up for various POC applications due to elimination of pressure-driven flows (Fig. 18.2.1).

The integrated CMOS-controlled fluid flow with AC electro-osmosis as well as cell manipulation and detection methods are represented in Fig. 18.2.2. Pressure-free electro-kinetic flow in a microfluidic system can be achieved in an electrolytic fluid by creating an electric field that cause a drag effect on the ions that are formed on electric double layer surface [6]. With a DC electric field, the voltages required to move the fluid scales with the length of the channel and can reach 100V for 100µm channels. To allow large-scalability of CMOS-driven microfluidics, we employ AC electro-osmosis that relies on a periodic arrangement of differentially driven asymmetric electrodes. As shown in Fig. 18.2.2, the differential voltages across the asymmetrical electrodes establishes a highly non-uniform electric fields, creating lateral drag forces on the ions locating on the electric double layer and thereby moving the bulk solution. Fig. 18.2.2 demonstrates a simulation of fluid flow in a microfluidic channel with ±9V differential voltage drives. In this work, the geometry of electrodes (fabricated with gold on glass) are optimized to enable velocity reaching 50-to-160µm/sec for 0.1-to-1mM ionic concentrations.

Enabled with CMOS driven flow, the cells in the sample can be subsequently manipulated, classified and then separated with DEP by a set of electrodes as shown in Fig. 18.2.2. The microfluidic system encompasses an altogether 7 pairs of focusing electrodes fabricated on both sides of the microfluidic channel. The reconfiguration of the excitation voltages on the top and bottom electrodes offers the ability to focus the cells anywhere across the vertical width of the channel, allowing precise control of their flow for robust impedance detection by the next set of 4 electrodes. A set of 4-element array impedance spectroscopy receiver allows near real-time detection and classification of the cell flow. For subsequent analysis and sorting, we employ another set of 7 pairs of electrodes that can channel the cell flow, separating them from the sample and the target molecules by only applying differential signals on either side of the electrodes (Fig. 18.2.2).

The architecture and the constituent circuits for the CMOS chips for fluid flow and cell/bio-molecule sensing are shown in Fig. 18.2.3. The chip integrates a total of 16 dedicated impedance spectroscopy receivers (12 for protein sensing and 4 for cell sensing). The excitation signal is synthesized by dividing an external LO signal and allow on-chip I,Q generation. The spectroscopic signals are processed through direct-conversion receivers that consists of multiplexed TIAs, passive mixers with quadrature LO drives and shared VGA and low-pass filters. The CMOS IC also integrates a set of 4 driving circuitries that allow AC-osmotic flow, focusing and cell separation with DEP. A 20MHz ring oscillator with a 16-bit counter enables a programmable drive capability for both osmotic flow and cell manipulation. To provide sufficient driving capabilities (up to 9V), we employ high voltage level shifters and drivers capable of operating across 5-9 V, which are shown in Fig. 18.2.3 with stacked 3.3V FETs. While AC osmosis requires an additional set of external amplifiers, each on-chip HV driver is able to provide two sets of HV differential signals for focusing and sorting the cells with DEP.

The measurement of the CMOS driven bulk fluid flow across several ionic concentrations and several electrode geometries is shown in Fig. 18.2.4. As expected, the measurement demonstrates that with the optimal geometry of the electrode (#1 pattern) and frequency (100KHz), the system has the ability to drive bulk fluid flow achieving a velocity up to 160µm/s. Also, the velocity expectedly has a nonlinear dependence on the amplitude drive and peaks for 0.001× PBS concentration (~0.1mM). Figure 18.2.5 demonstrates the characterizations for the cell focusing and sorting functionalities. As shown in the figure, the cell separation quality increases with voltage differentials across the electrode and reaches nearly 100% with 14Vpp applied to the upper electrodes from the CMOS IC drivers. The measurement of the focusing demonstrates that through controlled amplitudes of the driving signals on the top and bottom set of electrodes, the system can precisely focus cells in a streamline (within ±3µm for central flow) for robust subsequent detections.

Figure 18.2.6 shows the measured performance of the impedance spectroscopy for cells and proteins. The receiver achieves an input referred integrated noise of 301pA$_{rms}$ under 10Hz with a measured 95dB of dynamic range at 500kHz. Real-time cytometry measurements show the detection capability with 10µm and 20µm polystyrene beads, and S. Cerevisiae yeast cells. Expectedly, the signal strength increases with bead size. Also, it can be observed that under the controlled electronic focusing, cells are channeled closer to TIA input electrodes and the input signals are noticeably stronger than when they are further away (Fig. 18.2.6). Finally, label-free impedance immunosensor is performed on Au electrodes fabricated on silicon substrate across target concentrations of 20-to-100nM (Fig. 18.2.6). The Au surface was functionalized following thiol-modified chemistry by preparing a mixed self-assembled monolayer (SAM), which is employed for the antibody immobilization. The comparisons of the presented work with CMOS-based biosensing are shown in Fig. 18.2.7, demonstrating, for the first time, a scalable and programmable CMOS-driven pneumatic-free electro-kinetic flow with both cell manipulation, sensing and label-free sensing capabilities.

Acknowledgement:
The authors would like to thank National Science Foundation and Princeton Catalysis Institute for funding support, and all members of the IMRL lab for technical discussions.

References:
[1] T. Hunt, D. Issadore and R. Westervelt, "Integrated circuit/microfluidic chip to programmably trap and move cells and droplets with dielectrophoresis," *Lab on a Chip*, vol. 8, no. 1, pp. 81-87, 2008.
[2] C. Zhu et al., "A Packaged Ingestible Bio-Pill with 15-Pixel Multiplexed Fluorescence Nucleic-Acid Sensor and Bi-Directional Wireless Interface for In-Vivo Bio-Molecular Sensing," *IEEE Sym. VLSI Circuits*, pp. 1-2, June 2020.
[3] H. Tang et al., "2D Magnetic Sensor Array for Real-time Cell Tracking and Multi-site Detection with Increased Robustness and Flow-rate," *IEEE CICC*, pp. 1-4, Apr. 2019.
[4] L. Hong et al., "Fully Integrated Fluorescence Biosensors On-Chip Employing Multi-Functional Nanoplasmonic Optical Structures in CMOS," *IEEE JSSC*, vol. 52, no. 9, pp. 2388-2406, Sept. 2017.
[5] A. Manickam et al., "A CMOS Electrochemical Impedance Spectroscopy Biosensor 5array for Label-Free Biomolecular Detection," *ISSCC*, pp. 130-131, Feb. 2010.
[6] V. Studer et al., "An integrated AC electrokinetic pump in a microfluidic loop for fast and tunable flow control," *The Analyst*, vol. 129, no. 10, pp. 944-949, 2004.
[7] K. Lee et al., "A CMOS Impedance Cytometer for 3D Flowing Single-Cell Real-Time Analysis with ΔΣ Error Correction," *ISSCC*, pp. 304-305, Feb. 2012.
[8] M. Carminati et al., "Miniaturized Impedance Flow Cytometer: Design Rules and Integrated Readout," IEEE *TBioCAS*, vol. 11, no. 6, pp. 1438-1449, Dec. 2017.
[9] J. Chien and A. M. Niknejad, "Oscillator-Based Reactance Sensors with Injection Locking for High-Throughput Flow Cytometry Using Microwave Dielectric Spectroscopy," *IEEE JSSC*, vol. 51, no. 2, pp. 457-472, Feb. 2016.

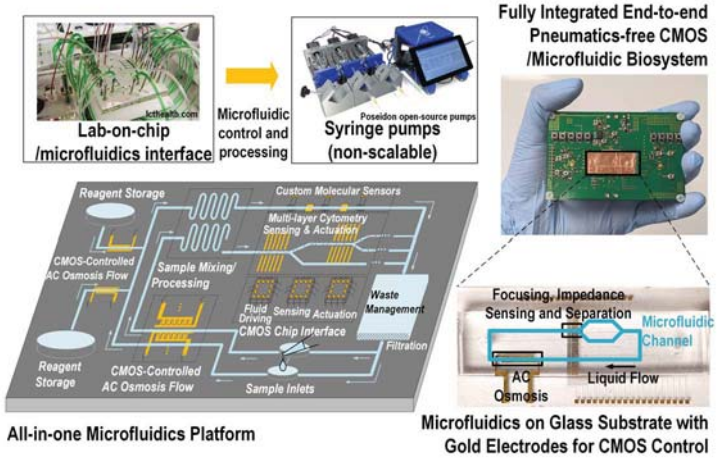

Figure 18.2.1: Fully integrated pneumatic-free CMOS driven/controlled microfluidics with label-free cell and bio-molecular sensing capabilities in CMOS IC for an end-to-end hybrid point-of-care system.

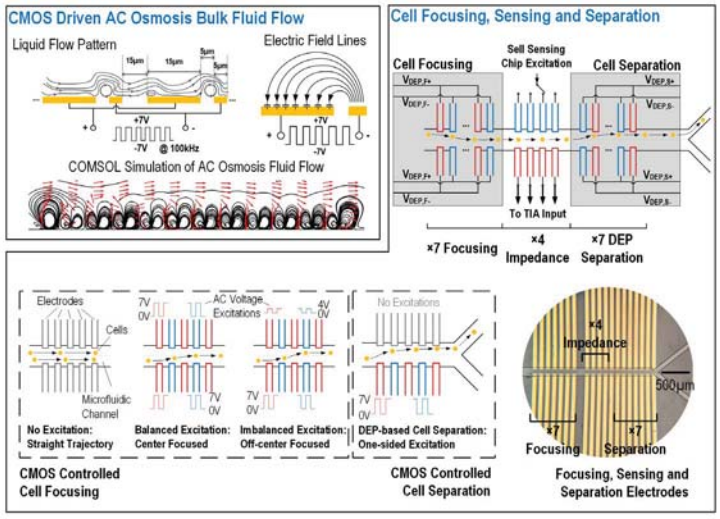

Figure 18.2.2: Integrated CMOS-controlled bulk fluid flow with AC osmosis and electronic cell focusing, sensing and separation methods.

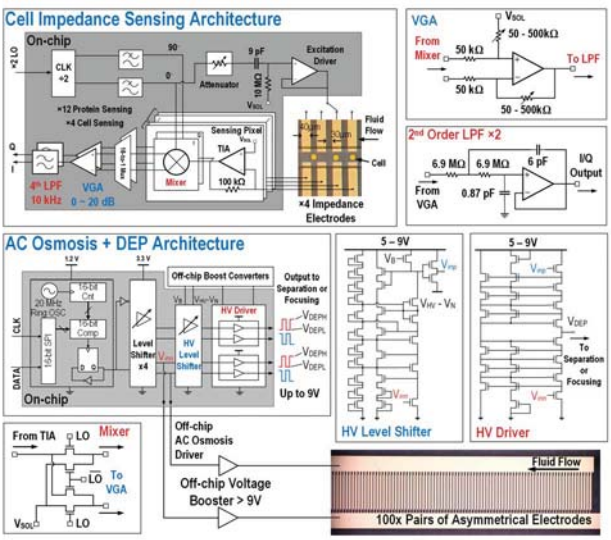

Figure 18.2.3: System architecture and constituent circuits for cell/protein impedance spectroscopy sensing as well as driver circuitries for bulk fluidic motion control with AC osmosis and cell manipulations with DEP.

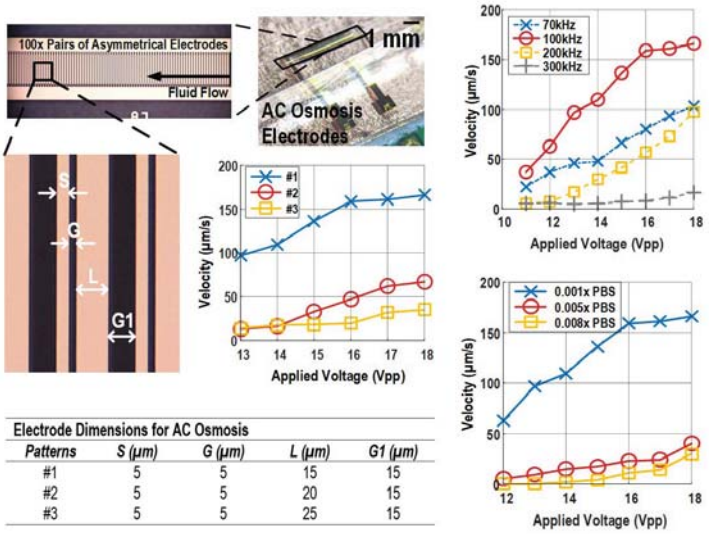

Electrode Dimensions for AC Osmosis

Patterns	S (μm)	G (μm)	L (μm)	G1 (μm)
#1	5	5	15	15
#2	5	5	20	15
#3	5	5	25	15

Figure 18.2.4: AC osmosis measurement results with different electrode patterns (100kHz), excitation frequencies (both under same 0.001X PBS concentration) and varying PBS concentrations (100kHz).

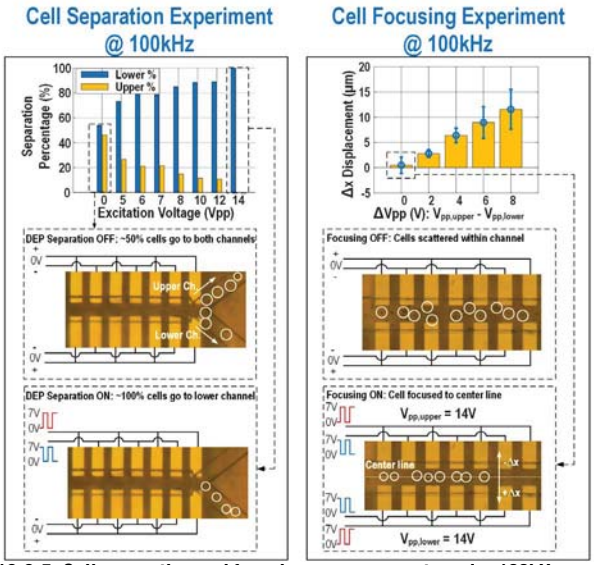

Figure 18.2.5: Cell separation and focusing measurements under 100kHz excitation frequency.

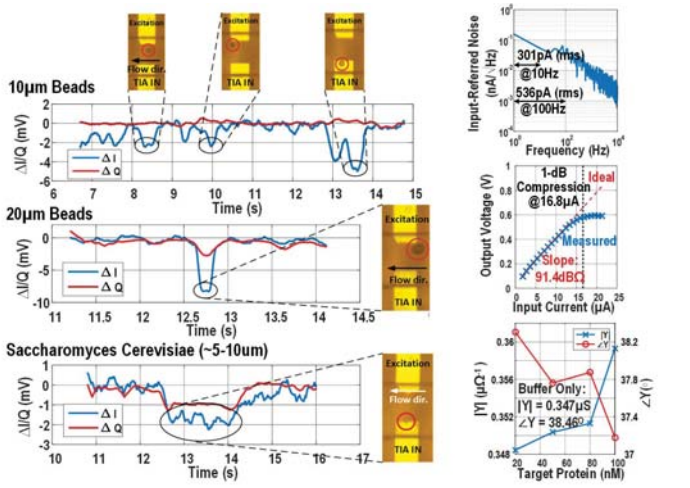

Figure 18.2.6: Impedance cytometry measurements of 10 and 20μm polystyrene beads and S. Cerevisiae showing ΔI & Q in real-time against solution baseline. TIA noise and linearity characterization achieves 95dB of dynamic range (500kHz). Label-free cytolysin toxin immunoassay is performed with 20-to-100nM of target concentration range.

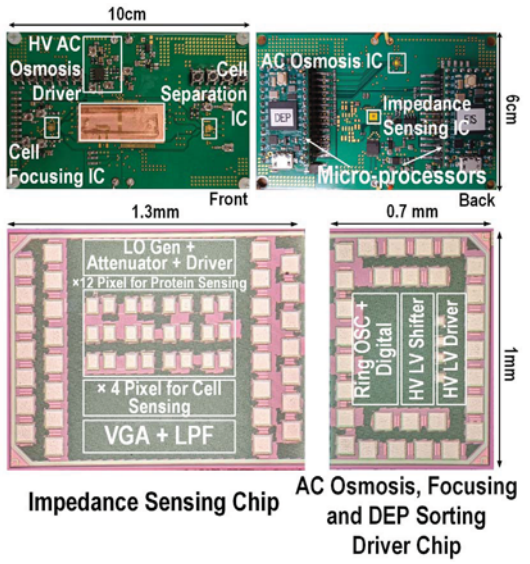

	This Work	K. Lee ISSCC 2012 [7]	M. Carminati TBioCAS 2017 [8]	J. Chien JSSC 2016 [9]	A. Manickam ISSCC 2010 [5]
Functionalities	**CMOS-driven bulk flow + cell focusing + 16-element impedance spectroscopy (4 cell, 12 protein)**	Pressure-driven flow + 2-element impedance spectroscopy	Pressure-driven flow + 1-element impedance spectroscopy	Pressure-driven flow + 4-element microwave dielectric spectroscopy	Protein + DNA impedance spectroscopy in static well
Process	**65nm**	N.A.	0.35μm AMS	65nm	0.35μm
Sensor Type	**On-chip TIA + direct conversion**	On-chip TIA + direct conversion	Off-chip TIA + direct conversion	Capacitive + High freq. oscillator	On-chip TIA + direct conversion
Integrated Bulk Fluid Control	**Yes**	No	No	No	No
Cell Focusing Method	**Integrated electronic DEP focusing**	External hydrodynamic focusing	External hydrodynamic focusing	External hydrodynamic focusing	N.A.
Cell Separation /Actuation	**Integrated CMOS-driven DEP separation**	No	Externally-driven DEP separation	No	N.A
Integrated Molecular Sensing	**Yes**	No	No	No	Yes
Power Consumption	**250μW/pixel**	N.A.	N.A.	65mW	720μW/pixel
Input Referred Noise	**301pA$_{rms}$ @ 10Hz**	N.A.	N.A.	N.A.	330pA$_{rms}$ @ 10Hz
Sensor Dynamic Range	**95dB**	N.A.	N.A.	N.A.	97dB
Cell Measurement	**S. cerevisiae**	RBC	S. cerevisiae	Polystyrene beads only	N.A.

Figure 18.2.7: Packaged external pneumatic-free biosystem. Impedance sensing chip and AC osmosis, focusing and DEP sorting chip die micrograph. Comparisons of the presented work with state-of-the-art cytometry sensors and impedance spectroscopy bio-molecular sensing platforms.

978-1-7281-9549-0/21/$31.00 ©2021 IEEE